Anal Bioanal Chem (2011) 401:817–825
DOI 10.1007/s00216-011-5088-y

ORIGINAL PAPER

3D configuration of mandibles and controlling muscles in rove beetles based on micro-CT technique

Dee Li · Kai Zhang · Peiping Zhu · Ziyu Wu · Hongzhang Zhou

Received: 17 January 2011 / Revised: 26 April 2011 / Accepted: 8 May 2011 / Published online: 22 May 2011

Abstract X-ray micro-CT is a powerful tool to visualize without damage details of the inner structures of beetles, the largest order of insects with a hard external skeleton. This contribution shows the three-dimensional (3D) reconstruction of the head morphology of three rove beetle species (Insecta, Coleoptera, Staphylinidae)—*Noddia* sp., *Creophilus maxillosus*, and *Hesperosoma* sp.—using X-ray microtomography at a spatial resolution of 6 μm. The details of skeletal muscle fiber insertions are described, giving a comprehensive overview of mandible mobility and organization. With the support of 3D rendering, we discuss the relationship among the mandible forms, the development of the muscles controlling the movement, and the head morphology. The well-developed posterior part of the head capsule is always accompanied by a well-developed mandible, a large adductor muscle, and a large apodeme for the wide areas of the muscle fiber attachment. In *Noddia* sp., muscles connected to the posterolateral angle of the head capsule are mainly short muscles, whereas in *Creophilus maxillosus*, the latter are mainly long muscles, and in *Hesperosoma* sp. no mandible adductor muscle fibers are present on the posterolateral angle of the head capsule. These results offer new invaluable information regarding the biting functions of beetle mandibles and the trend of their morphological change during their long-term evolution.

Keywords Mandible · Mandible muscles · Three-dimensional reconstruction · Head capsule · Staphylininae

Published in the special issue *Imaging Techniques with Synchrotron Radiation* with Guest Editor Cyril Petibois.

Awarded an ABC Poster Prize on the occasion of the 3rd International Workshop on Imaging Techniques with Synchrotron Radiation, held in Suzhou, China.

D. Li · H. Zhou (✉)
Key Laboratory of the Zoological Systematics and Evolution,
Institute of Zoology, Chinese Academy of Sciences,
1 Beichen West Road, Chao Yang,
Beijing 100101, China
e-mail: zhouhz@ioz.ac.cn

K. Zhang · P. Zhu · Z. Wu (✉)
Beijing Synchrotron Radiation Facility,
Institute of High Energy Physics, Chinese Academy of Sciences,
Beijing 100049, China
e-mail: wuzy@ustc.edu.cn

Z. Wu
National Synchrotron Radiation Laboratory,
University of Science and Technology of China,
Hefei 230026, China

D. Li · K. Zhang
Graduate School of the Chinese Academy of Science,
19 Yuquan Road, Shijingshan,
Beijing 100039, China

Introduction

The rove beetles (Insecta, Coleoptera, Staphylinidae) are mainly predators and their heads are mostly prognathous in form. They use the mandible of their mouthparts to bite food in the form of very small invertebrate animals, penetrating body walls characterized by different toughness and strength. As a result of a long-term adaptation to this function, the evolution of rove beetle mandibles shows different modifications useful for species identification and

classifications [1]. According to previous morphological studies [1–5], three different types of mandibles and heads can be recognized: well-developed mandibles inserted on the head capsule with large and prominent temples (the region between compound eyes and the morphological cervix); a developed mandible inserted on the head capsule with small and curved temples; weakly developed and falciform mandibles inserted on the head capsule with round temples. Some phylogenetic studies tried to explain the differentiation phenomenon with independent origins and isolated evolutions [6, 7]. Presently, the relationship of the head shapes and the robustness of mandibles in rove beetles as well as in other beetle groups is a matter of debate [8–10].

A pair of mandibles is usually located in front of the head and each mandible is articulated by a pair of condyles, i.e., the dorsal and the ventral condyles. The pair of mandibles can swing inward and outward in the biting movement as forceps, around the axis formed by the two condyles [2, 11]. The mechanical strength of the beetle mandibles depends by the muscle fiber organization with respect to the different levers (distances between insertions and articulations). This biting movement is controlled by two muscles (or fiber groups of muscles), the mandible adductor and the abductor muscles [12]. The mandible adductor muscle fibers are connected to the apodeme in the proximal ends, which conveys forces to the mandible base [9]. The distal ends of mandible muscles are linked to the posterior part of the head capsule [12, 13]. Owing to different predatory behaviors and foods, the development of the mandible and their attachment muscles can be differentiated. Correspondingly, the morphology of the posterior part of the head is never the same, with a different extent of development of the mandibles and of their muscles [14]. Wheater and Evans [10] tried to identify a relationship between the head width, the mandible tip area or the adductor muscle attaching area on the apodeme, and the mandible force of some beetle species. They found a significant relationship between the mandible strength and the adductor muscle attaching area on the apodeme. Another study performed on some water beetle species (Dytiscidae) showed that the widening posterior region of the cranium is due to the increase of the mandible adductor muscle during ontogeny [15, 16]. Studies with ants also revealed that fast mandible movements usually featured long heads and small apodeme attaching angles, whereas forceful mandible movements feature broad heads [8, 9]. However, width and length are both not the most suitable characteristics to use when monitoring the mandible shapes and to explain the complex relationship among mandible shapes and head morphology, an issue still poorly understood. Earlier studies attempted to calculate the volume of the head and the adductor muscle and the apodeme areas [8, 9, 17]. Moreover, phylogenetic and morphological studies tried to deal with the head morphology of rove beetles on the basis of two-dimensional (2D) data [2–7, 18]. Gorb and Beutel [14] studied the head capsule design and the mandible control in beetle larvae using a three-dimensional (3D) approach. However, their measurements of the head performed using a light microscope were not sufficient to achieve a conclusion and only 3D results obtained with micro-CT proved to be useful for reconstructing the morphology of beetle heads [19, 20].

Although already a well-recognized method, X-ray tomography has been significantly improved recently. It has already been applied to reconstruct insect morphology because of the nondamaging character, the reliability, and the high spatial resolution [14, 20–22]. The great advantage is, however, that it does not require specimen dissections and insects can be preserved after observations [23]. This is particularly important for the investigation of internal tissues. With X-ray tomography, entomologists may really get access to the internal morphology of an insect. Moreover, the use of micro-CT allows imaging of a small specimen with spatial resolution in the range 1–50 μm, values that fit well within the dimensions of typical skeletal muscles of the mandible articulations. Skeletal muscle fibers of insects have a typical diameter of approximately 20 μm and are 100–1,000 μm long. To find the relationship between the mandible morphology, mandible muscles, and the head capsule, using micro-CT we performed a 3D reconstruction of the head morphology of three rove beetles with three different mandible types, i.e., the robust, the developed, and the falciform mandible. Most of the size evaluations, e.g., length, width, area, and volume of different tissues, were obtained with the Amira 4.1 software package. The main goal was to identify a relationship between the shape of the mandible, the development of controlling muscles, and the morphology of the posterior part of the head.

Materials and methods

The three rove beetle species selected in this study are *Noddia* sp., *Creophilus maxillosus*, and *Hesperosoma* sp. Specimens were preserved in the collection in 75% alcohol before undergoing to a special treatment. For X-ray tomography experiments, specimens were treated in Dubosque–Brazil solution for 2 days, then transferred to 100% alcohol gradually and dried in a critical point dryer (HCP-2). All measurements and reconstructions were performed at the Institute of High Energy Physics of the Chinese Academy of Sciences using a MicroXCT-200 system, manufactured by Xradia (USA). The typical MicroXCT 200 system shown in Fig. 1 consists of a

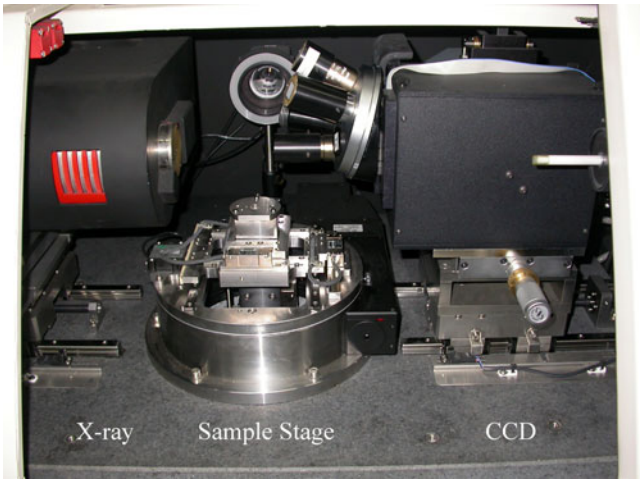

Fig. 1 The setup of the MicroXCT-200 system

sealed microfocus X-ray tube (40–150 keV, 5-μm spot size), a fiber optic coupled to a cooled CCD detector, and a precision sample stage to align the specimen. A dual-processor computer was also used to steer stepping motors, axial shift, and data recording, as well as to reconstruct CT images.

Experiments were performed by placing the insect on the sample stage between the X-ray source and the CCD detector. The photon energy used was 40 keV and the source-to-sample distances were 39, 89, and 39 mm for *Noddia* sp., *Creophilus maxillosus*, and *Hesperosoma* sp., respectively. As the source produces a divergent X-ray beam, the magnification was achieved by moving the object toward the X-ray source. After the alignment, 2D X-ray images were collected in 361 angular positions in a range of 180° with an exposure time of 10 s each. The total exposure time and the scan time were 60 and 70 min, respectively. The cross sections of the object were reconstructed by applying the "filtered back-projection algorithm for fan-beam geometries." This algorithm combines all angular information for every slice in the camera to generate a cross section of the object. In total, 1,024 cross sections of the object were reconstructed with a lateral resolution and a slice-to-slice distance of the order of few micrometers. The detection chain was completed by a 20-μm YAG-Ce scintillator, an optical microscope (with magnification ranging between ×1 and ×40), and a low-noise fast-readout 2,048×2,048 pixels CCD with 16-bit dynamic range. To obtain the 3D inner structure of *Noddia* sp., *Creophilus maxillosus*, and *Hesperosoma* sp., a magnification factor of 2 was used, corresponding to effective pixel sizes of 5.97, 11.62, and 5.37 μm, respectively. Finally, 3D reconstruction and analysis of the X-ray data was done with the Amira 4.1 software package running on a Xeon 2660 MHz computer.

Results and discussion

Mandible and head capsule

The three species studied, whose mandibles change from well to weakly developed characters, belong to the subfamily of the Staphylininae (Insecta, Coleoptera, Staphylinidae). The mandible of *Noddia* sp. is short and robust with a thin prostheca (Fig. 2C–E). The mandible of *Creophilus maxillosus* is thinner than that of *Noddia* sp. and well developed without prostheca (Fig. 2H–J), whereas the mandible of *Hesperosoma* sp. is the thinnest and longest in the three species and falciform without prostheca (Fig. 2M–O). The volume ratio of the mandible to the half head capsule is 27.77, 21.33, and 21.45 in *Noddia* sp., *Creophilus maxillosus*, and *Hesperosoma* sp., respectively, i.e., from the well to the weakly developed component.

The head capsule of *Noddia* sp. is subquadrangular in the dorsal view, and gradually broadens at the posterior end in the ventral view, being broadest to the posterior end. The compound eyes are small, protruding laterally, and not detectable in the ventral view. The temple is long with protruding posterior angles. The morphological cervix is semicircular in the dorsal view (Figs. 2A, B, 3A–C). The head capsule of *Creophilus maxillosus* is rounded in the dorsal view and subquadrangular in the ventral view, being broadest just at the posterior of the compound eyes. The compound eyes are large, flat, and not detectable in the ventral view. The temple is shorter than the compound eye with a rounded posterior angle. The cervix is broad and semicircular in the dorsal view (Figs. 2F, G, 3D–F). The head capsule of *Hesperosoma* sp. is subquadrangular in the dorsal view, being broadest at the anterior end. The compound eyes are small, weakly protruding, and detectable in the ventral view. The temple region is long but flatter than in the other two species. The cervix is narrow and subquadrangular in the dorsal view (Figs. 2K, L, 3G–I).

The head capsules of insects are part of the external skeleton and they make impossible the observation of inner organs and tissues within the capsules unless a destruction of the head capsule is considered. Because of the irregular shape of the head and muscles, evaluations are necessary to calculate the muscle attaching area on the head capsule, the volume of the head capsule, the surface area of the apodeme, and the angles between muscle fibers and the apodeme [8, 9, 17]. Using imaging is fundamental for the reliability of the results achieved and for the selection of the best method to measure the above-mentioned geometrical parameters. In our study, we obtained these morphological values directly using Amira 4.1, i.e., distances, surface areas, volumes, and angles. Moreover, because of the advantages of no damage and the absence of artifacts, a lot of morphological or phylogenetic studies of the head

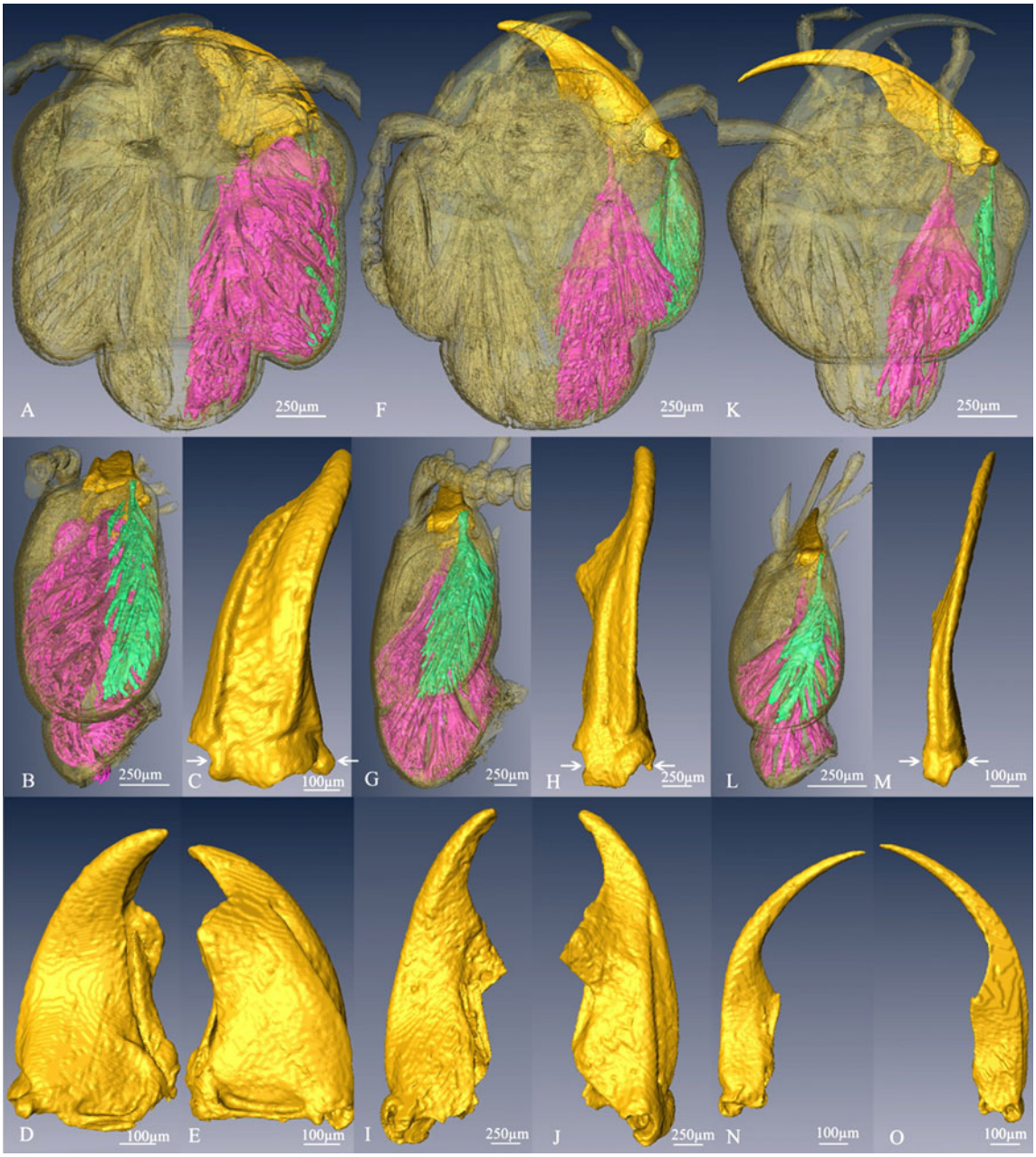

Fig. 2 Three dimensional reconstructions of *Noddia* sp. (**A**–**E**), *Creophilus maxillosus* (**F**–**J**), and *Hesperosoma* sp. (**K**–**O**). **A**, **B**, **F**, **G**, **K**, **L** Head, transparent view; mandible and mandible muscles, shade view; **A**, **F**, **K** dorsal view; **B**, **G**, **L** lateral view. **C**–**E**, **H**–**J**, **M**–**O** Mandible, shade view; **C**, **H**, **M** lateral view; **D**, **I**, **N** ventral view; **E**, **J**, **O** dorsal view. *Purple* the mandible closer muscle, *green* the mandible opener muscle. *Arrows* show mandible insertions with the head capsule. Between arrows we show the mandible rotation axis

were based on micro-CT data [8, 19–22]. However, using the X-ray micro-CT method, we attempted to investigate the mechanism underlying the mandible movement and the relationship between skeleton and muscles.

Mandible muscles and muscle attachments

There are two groups (or fibers) of muscles controlling the movement of the mandible: the mandible adductor and the mandible abductor muscle, named in Latin *musculus craniomandibularis internus* and *musculus craniomandibularis externus*, respectively. The mandible adductor muscle is well developed and much larger than the mandible abductor muscle (Figs. 2B, G, L, 4A, B, D, E, G, H). The volume ratios of the adductor to the abductor muscles are 12.24, 6.40, and 5.40 in *Noddia* sp., *Creophilus maxillosus*, and *Hesperosoma* sp., respectively. The volume ratios of the adductor muscle to the half head capsule are 32.69,

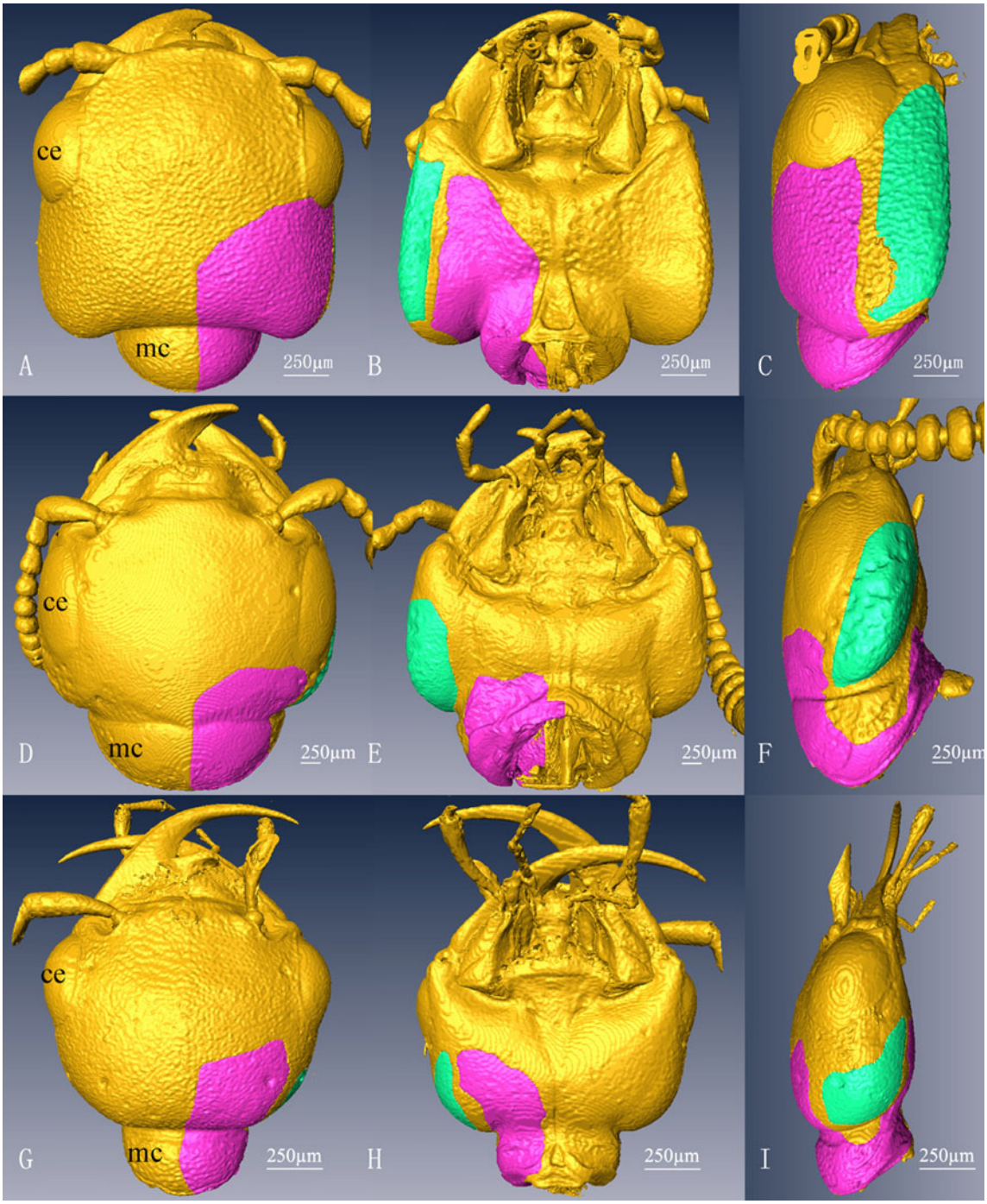

Fig. 3 Three-dimensional reconstructions (shade view) of *Noddia* sp. (**A**–**C**), *Creophilus maxillosus* (**D**–**F**), and *Hesperosoma* sp. (**G**–**I**). **A**, **D**, **G** Dorsal view. **B**, **E**, **H** Ventral view. **C**, **F**, **I** Lateral view. *Purple* attaching area of the mandible closer muscle, *green* attaching area of the mandible opener muscle, *ce* compound eye, *mc* morphological cervix

25.93, and 30.46 in *Noddia* sp., *Creophilus maxillosus*, and *Hesperosoma* sp., respectively, whereas the volume ratios of the abductor muscle to the half head capsule are 9.52, 8.13, and 6.27 in *Noddia* sp., *Creophilus maxillosus*, and *Hesperosoma* sp., respectively. In the three species studied, a well-developed mandible is accompanied by a large adductor muscle volume, whereas a weakly developed mandible is accompanied by a small adductor muscle volume.

The mandible adductor and abductor muscles are linked to the external and internal proximal angles of the mandible, respectively (Figs. 2A, F, K, 4A, B, D,

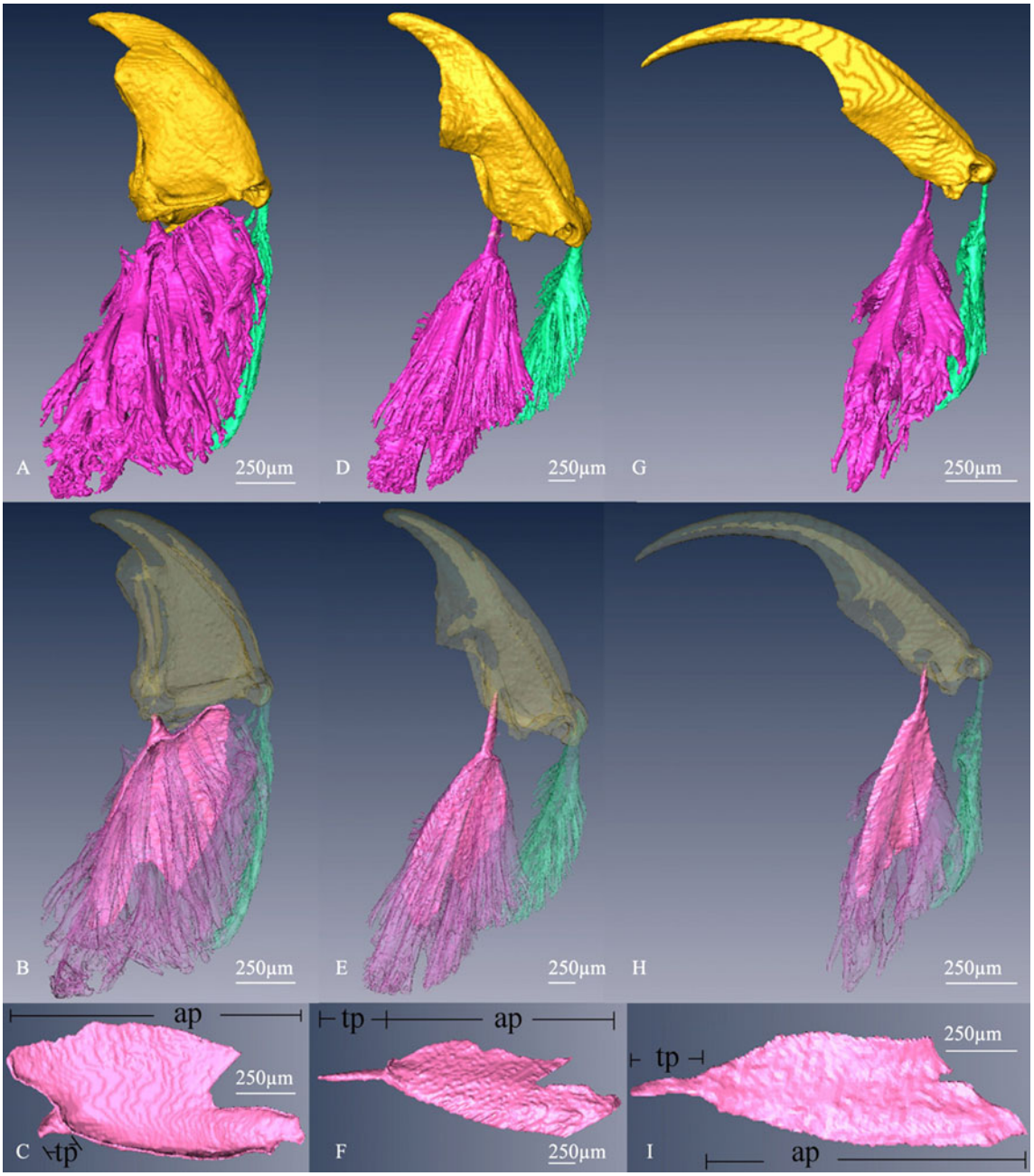

Fig. 4 Three-dimensional reconstructions of *Noddia* sp. (**A**–**C**), *Creophilus maxillosus* (**D**–**F**), and *Hesperosoma* sp. (**G**–**I**). **A**, **D**, **G** Mandible and mandible muscles, shade view. **B**, **E**, **H** Mandible and mandible muscles, transparent view; the apodeme of the mandible closer muscle, shade view. **C**, **F**, **I** The apodeme of the mandible closer muscle, shade view. *Purple* the mandible closer muscle, *green* the mandible opener muscle, *pink* the apodeme, *ap* attaching part, *tp* transmitting part

E, G, H). The mandible adductor muscle originates from the posterodorsal and posteroventral head capsule and morphological cervix, whereas the mandible abductor muscle originates from the temple region posterior to the compound eye. Figure 3 also shows the muscle attaching area on the head capsule of the three species. In *Noddia* sp., the links of the adductor muscle are just posterior to the compound eye dorsally and dorsolaterally, and on most of the postgenal plate and inner sides of the morphological cervix. The links of the abductor muscle are on the ventrolateral angle of temple and the ventral and posteroventral sides of the compound eye (Fig. 3A–C). In *Creophilus maxillosus*, the links of the adductor muscle are dorsally on the posterior part of the compound eye and ventrally on the posterior part of the postgenal plate and on the inner sides of the cervix. The

links of the abductor muscle are ventral and posteroventral to the compound eye and on the temple regions (Fig. 3D–F). In *Hesperosoma* sp., the links of the adductor muscle are dorsally on the posterior part of the head at a short distance from the compound eye, and ventrally on the posterior part of the postgenal plate and on the inner sides of the cervix. The connections of the abductor muscle are on the posterior part of the temple and are also a short distance from the compound eye (Fig. 3G–I). The ratio of the adductor muscle area to the surface area of the half head capsule (the area of the head for muscle attachments) is 38.03, 28.32, and 32.24 in *Noddia* sp., *Creophilus maxillosus*, and *Hesperosoma* sp., respectively. The ratio of the abductor muscle area to the surface area of the half head capsule is 10.85, 10.63, and 7.55 in *Noddia* sp., *Creophilus maxillosus*, and *Hesperosoma* sp., respectively. Knowledge of only the muscle attachment area on the head capsule is not enough to understand the relationship among mandible, mandible muscles, and head capsule. The mandible connecting angles also have to be considered.

As is well know, the mandible adductor muscle has the function to close the mandible and snapping prayers in the rove beetle. The mandible swings inward and outward around the axis formed by the dorsal and the ventral condyles of the mandible. Paul [8] introduced a biomechanical model to explain the relationship between the mandible strength and the head capsule volume. The mandible movement mechanism of ants and other species were also studied [24, 25]. We attempted to obtain a relationship between the mandible shape and the mandible strength. The adductor muscle strength is equal to the force at the mandible apex produced by snapping (Fig. 5). Let us now suppose that the direction of the force of the mandible apex is always applied along the tangent of the apex. As a result, we may write

$$FH\sin\alpha = fL\cos\beta,$$

where F is the force produced by the mandible adductor muscle, H is the length of the lever arm of the adductor muscle, α is the angle between the adductor muscle and the lever arm, f is the force transmitted to the apex of the mandible, L is the distance between the apex of the mandible and the axis, and β is the angle between the apex of the mandible and the mandible axis.

We used the volume ratio of the adductor muscle to the half head capsule to describe F, whereas we used the length ratio of the mandible with respect to the lever arm of the abductor muscle to represent L. We measured the variations of the three specimens on the basis of 3D data from micro-CT and calculated the force transmitted from the adductor muscle to the apex of the mandible (f). The f value of *Noddia* sp. is

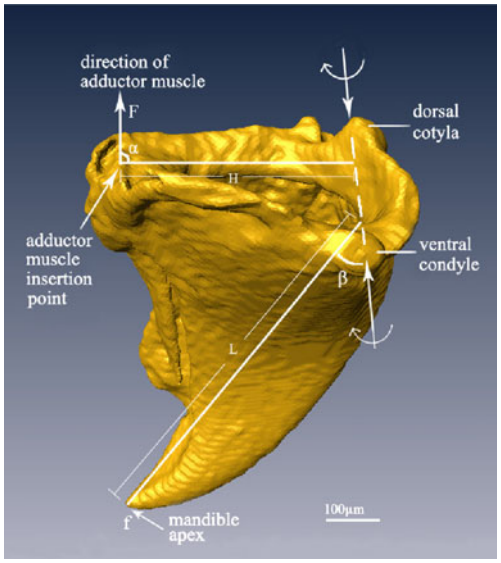

Fig. 5 Measurements of the mandible. The *arrows* between mandible insertions show the mandible rotation axis; the *circular arrows* centered on the rotation axis show the rotation direction of the mandible generated by the axis

5.82 times greater than that of *Hesperosoma* sp., whereas the f value of *Creophilus maxillosus* is 1.67 times greater than that of *Hesperosoma* sp. In addition, we supposed the strength of the adductor muscle (F) to be constant for the same species. The force transmitted to the apex of the mandible (f) will increase as the lever arm of the adductor muscle (H) increases with a linear relationship, so (Fig. 6A)

$$f = (F\sin\alpha/L \cdot \cos\beta)H.$$

As a result, the slope gradually decreases in *Noddia* sp., *Creophilus maxillosus*, and *Hesperosoma* sp. respectively. The force transmitted to the apex of the mandible (f) will decrease, increasing the length between the apex of the mandible and the swinging axis (L), giving (Fig. 6B)

$$f = (FH\sin\alpha/\cos\beta)\frac{1}{L}.$$

The force transmitted to the apex of the mandible (f) will decrease, increasing the angle between the apex and the axis of the mandible. Then (Fig. 6C),

$$f = (FH \cdot \sin\alpha/L)\frac{1}{\cos\beta}.$$

The mandible of *Noddia* sp. is broad and robust; its mandible adductor muscle is well developed, resulting in a more powerful biting force. The mandible of *Hesperosoma* sp. is long and falciform, its mandible adductor muscle is weakly developed, and therefore it may produce a smaller biting force.

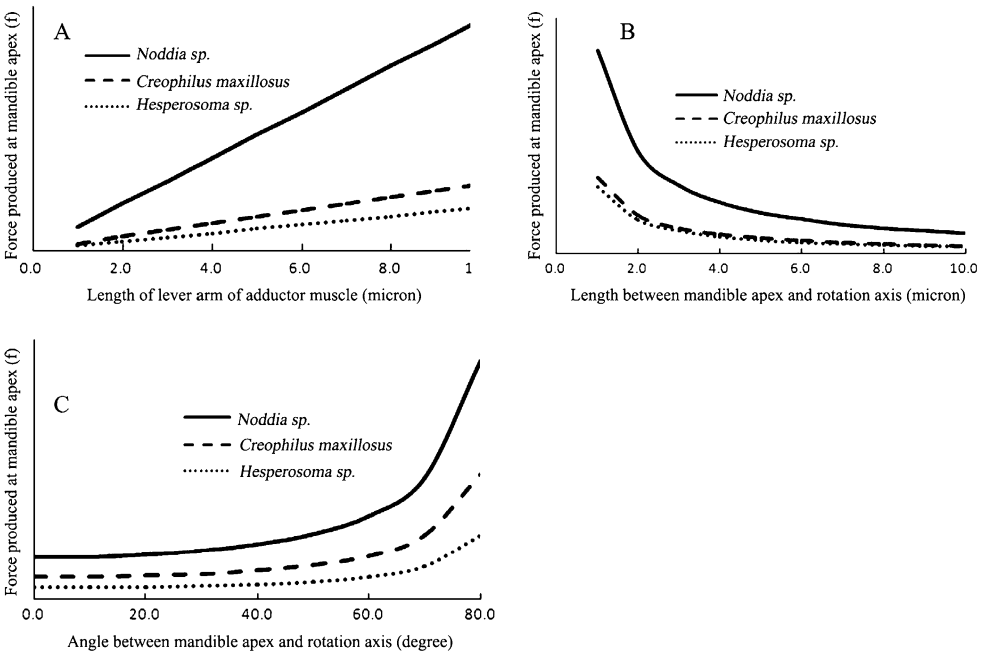

Fig. 6 Relationships between the mandible strength at the mandible apex (*f*) and the length of the lever arm of the adductor muscle (*H*) (**A**, cf. Fig. 5), the distance between the mandible apex and the rotation axis (*L*) (**B**, cf. Fig. 5), and the angle between the mandible apex and the rotation axis (β) (**C**, cf. Fig. 5)

Apodeme

There is an apodeme for each of the mandible adductor muscle fibers in the three beetle species studied, but there is no apodeme for mandible abductor muscle fibers. The apodeme of the mandible adductor muscles of the rove beetle is weakly sclerotized and can be divided into the anterior transmitting and the posterior attaching part. The anterior transmitting part is used to transmit forces to the mandible and it is cylindrical or flat without any muscle attachments, whereas the posterior attaching part is broad and thin to support muscle attachments (Fig. 4B, C, E, F, H, I). The apodeme of *Noddia* sp. is well developed. The anterior transmitting part is short and broad. The posterior attaching part is broad and bent upward along the inner margin. It is bilobed distally and protrudes anterolaterally, almost exceeding the transmitting part (Fig. 4C). The apodeme of *Creophilus maxillosus* is smaller than that of *Noddia* sp. The anterior transmitting part is long and cylindrical. The posterior attaching part bends downward at the inner margin. It is also bilobed distally and gradually narrowed forward (Fig. 4F). The apodeme of *Hesperosoma* sp. is weakly developed. The anterior transmitting part is flat and shorter than that of *Creophilus maxillosus*. The posterior attaching part is gradually narrowed forward, with a small depression distally (Fig. 4I). The ratio of the area of the apodeme (only the ratio for the posterior attaching part was calculated) to the surface area of the half head capsule is 19.50, 13.68, and 13.44 in *Noddia* sp., *Creophilus maxillosus*, and *Hesperosoma* sp., respectively.

There are two different types of mandible muscle fibers in the three species we studied: the muscle fibers originating from the dorsal and the ventral part of the head capsule, which are relatively short with an angle with the apodeme of approximately 45°; the muscle fibers originating from the morphological cervix, which are relatively long and with an angle with the apodeme smaller than 30°. However, the muscle fibers originating from the posterolateral angle of the head capsule are different in the three species we investigated. The angle of the muscles originating from the posterolateral protruding angle of the head is around 30° in *Noddia* sp. The muscles are mainly short (Fig. 4A–C). The angle of the muscles originating from the posterolateral angle of the head is less than 30° in *Creophilus maxillosus*. These muscles are mainly long muscle fibers (Fig. 4D–F). Finally, there is no muscle attaching on the posterolateral angle of the head capsule in *Hesperosoma* sp. (Fig. 4G, H).

The apodeme of the Staphylininae is well developed and sheetlike in shape. The optimum angles of the muscle fiber attachment range between 41° and 45° for maximum strength. The morphology of the apodeme and the muscle attaching angles are always species-specific [8, 9, 26]. For most of the fibers of the mandible adductor muscles of *Noddia* sp., the attaching angles are approximately 45°, whereas in the other two species, more long muscle fibers with smaller attaching angles occur. We may conclude that the strength is greatest in *Noddia* sp. We also found an interesting result connected with the adductor muscles. They are short muscles originating from the posterolateral angle of the head of *Noddia* sp.

and the angles with the apodeme are approximately 40°. The muscles are long muscles originating from the posterolateral angles of the head of *Creophilus maxillosus* and the angles with the apodeme are approximately 30°. In addition, there are no adductor muscles originating from the posterolateral angle of the head except for the mandible abductor muscle in *Hesperosoma* sp. As a consequence, the morphology of the posterior part of the head has a close relationship with the mandible and the mandible muscles. The organization and orientation between skeletal muscle fibers, tendons, and connective tissue (primarily made by a collagen network directed toward the tendons) is a critical feature to understand the power of small muscles. Unfortunately, 3D rendering obtained by micro-CT, although accurate, does not allow discrimination between muscles and connective tissues. Further studies possibly based on labeling of soft tissues will probably allow discrimination between the different components.

Conclusion

We presented an accurate nondamaging imaging investigation of the details of the inner structures of beetles, the largest order of insects with a hard external skeleton. Components can be correlated with the mandible movement and relationships based on these 3D reconstructions using micro-CT were obtained. The study showed that well-developed and robust mandibles are always present with well-developed adductor muscles and protruding temples. In contrast, weakly developed or falciform mandibles are correlated with weakly developed adductor muscles and short or rounded temples.

From the analysis we may claim that the force available to the apex of the mandible increases proportionally to the length of the lever arm of the adductor muscle, whereas the force available to the apex of the mandible decreases as the length between the apex of the mandible and the rotation axis increases. Finally, the force available to the apex of the mandible decreases as the angle between the apex and the axis of the mandible increases. A broad and short (robust) mandible with a sharp apex produces the greatest strength with the same force output of the mandible adductor muscle. 3D rendering obtained by micro-CT is extremely useful and offers accurate spatial information for the kinematic analysis of the mandible movement. The results obtained also provide valuable clues in the understanding of the evolution of the mouthpart and predating behavior of these beetles.

Acknowledgements We are very grateful to Augusto Marcelli (Istituto Nazionale di Fisica Nucleare, Frascati, Italy) and four anonymous reviewers for their valuable suggestions to improve the manuscript. This study was partly supported by the National Natural Science Foundation of China (NSFC-31071909, NSFC-J0930004), the Key Important Project of the National Natural Science Foundation of China (10734070), the National Key Technology R&D Program (2008BAC39B02), and the CAS Innovation Program (KSCX2-YW-Z-0910, KJCX2-YW-N42). The authors also acknowledge a grant from the Key Laboratory of Zoological Systematics and Evolution of CAS (no. O529YX5105).

References

1. Smetana A, Davies A (2000) Am Mus Novit 1–88
2. Blackwelder RE (1936) Smithson Misc Collect 94:102
3. Naomi S-I (1987) Kontytu 55:38–48
4. Naomi S-I (1987) Kontytu 55:28–36
5. Naomi S-I (1988) Kontytu 56:67–77
6. Beutel RG, Leschen RAB (2005) Syst Entomol 30:510–548
7. Hansen M (1997) Phylogeny and classification of the staphyliniform beetle families (Coleoptera). Det Kongelike Danske Videnskabernes, Copenhagen
8. Paul J (2001) Comp Biochem Physiol A Mol Integr Physiol 131:7–20
9. Paul J, Gronenberg W (1999) J Exp Biol 202:797–808
10. Wheater CP, Evans MEG (1989) J Insect Physiol 35:815–820
11. Manton SM, Harding JP (1964) Philos Trans R Soc Lond B Biol Sci 247:1–183
12. Kéler SV (1963) Entomologisches Wörterbuch. Akademie, Berlin
13. Snodgrass RE (1935) Principles of insect morphology. Cornell University Press, Ithaca
14. Gorb S, Beutel RG (2000) J Morphol 244:1–14
15. Barman EH (2005) Coleopt Bull 59:351–360
16. Barman EH (2004) Coleopt Bull 58:661–671
17. Barman EH, Wall WP, Mouton A, Fenn TR (2008) Coleopt Bull 62:279–286
18. Betz O, Thayer MK, Newton AF (2003) Acta Zool 84:179–238
19. Zhang K, Li D-e, Zhu P, Yuan Q, Huang W, Liu X, Hong Y, Gao G, Ge X, Zhou H, Wu Z (2010) Anal Bioanal Chem 397:2143–2148
20. Weide D, Betz O (2009) J Morphol 270:1503–1523
21. Beutel RG, Ge S-q, Hönschemeyer T (2008) Cladistics 24:270–298
22. Hörnschemeyer T, Beutel RG, Pasop F (2002) J Morphol 252:298–314
23. Betz O, Wegst U, Weide D, Heethoff M, Helfen L, Lee W-K, Cloetens P (2007) J Microsc 227:51–71
24. Gronenberg W, BrandÃO CRF, Dietz BH, Just S (1998) Physiol Entomol 23:227–240
25. Gautestad AO, Mysterud I (1993) J Appl Ecol 30:523–535
26. Gronenberg W, Paul J, Just S, Hölldobler B (1997) Cell Tissue Res 289:347–361